# Cyclic $CO_2$ Capture by Limestone-Derived Sorbent During Prolonged Calcination/Carbonation Cycling

**Ping Sun, C. Jim Lim, and John R. Grace**
Dept. of Chemical and Biological Engineering, University of British Columbia, Vancouver, Canada V6T 1Z3

*DOI 10.1002/aic.11491*
*Published online April 18, 2008 in Wiley InterScience (www.interscience.wiley.com).*

*The performance of limestone-derived CaO during many (>1000 in some cases) calcination and carbonation cycles is reported. After 150 cycles, the calcium utilization during carbonation reached a minimum value between 4 and 17%, with the asymptotic level depending strongly on the carbonation time. With the aid of mechanistic studies including investigations on sorbent surface topology by SEM and mercury intrusion, a mechanism for pore evolution during the cyclic capture is proposed consistent with the experimental observations.* © 2008 American Institute of Chemical Engineers *AIChE J,* 54: 1668–1677, 2008
*Keywords: $CO_2$ capture, calcination, carbonation, sorption, limestone sintering*

## Introduction

The utilization of calcium-based sorbents in looping cycles for the removal of $CO_2$ is a topic of worldwide attention due to the role of $CO_2$ in causing climate changes as a greenhouse gas. Different applications have been proposed, including $CO_2$ removal from steam reformers, gasifiers, and water-gas shift reactors where the carbonation reaction can improve hydrogen yields (Han and Harrison, 1994; Johnsen et al., 2006; Lin et al., 2001, 2002a; Ortiz and Harrison, 2001),[1–5] while also providing heat and facilitating $CO_2$ sequestration. Calcination/carbonation cycles are also of interest for fluidized bed combustors (Abanades et al., 2003, 2004a; Shimizu et al., 1999; Sun et al., 2007a–c).[6–11]

The decline in sorbent capability during multiple sorption/regeneration cycles, leading to a loss of reversibility, is a key issue in all such processes. The ultimate utilization determines the sorbent make-up rate required in any commercial plant, heavily influencing the cost of operation (Abanades et al., 2004b).[12] Limestones are superior to dolomites in price, abundance, and mechanical strength, but dolomites have generally been found to show less loss of reactivity than limestones (Silaban et al., 1996; Sun et al., 2007a)[9,13] over the limited number of cycles (typically 15–20) tested. Various natural limestones have usually been found to follow similar decay trends when exposed to cyclic capture conditions (Abanades 2002; Sun et al., 2007a).[9,14]

Sintering of CaO during calcination, indicated by the change of sorbent surface texture after multiple cycles, is believed to be the major cause of deactivation (Abanades and Alvarez, 2003; Borgwardt, 1989a,b; Sun, 2007; Sun et al., 2007a–d).[9–11,15–19] The surface texture of cycled limestones commonly features shrinkage of smaller pores, usually accompanied by growing macropores (Abanades and Alvarez, 2003; Sun et al., 2007a–d).[9–11,15,19] These trends are typical of solid-state sintering in an intermediate stage, as described by sintering theory (German, 1996)[20] in which vacancies (or voids) generated by temperature-and-ion-sensitive lattice defects direct void volume from smaller to larger pores, whereas mass moves in the opposite direction. Ionic compounds such as CaO mostly sinter due to a volume diffusion or a lattice diffusion mechanism (German, 1996).[20] A lattice diffusion control mechanism for CaO sintering has been confirmed experimentally by Borgwardt (1989a).[16] Both $CO_2$

Correspondence concerning this article should be addressed to C. Jim Lim at cjlim@chml.ubc.ca.

Current address of Ping Sun: Sherritt Technologies, 1600, 10235-101 St., Edmonton, Canada T5J 3G1.

and steam have been reported to enhance CaO sintering (Beruto et al. 1984; Borgwardt, 1989b; Ewing et al. 1979).[17,21,22]

Sun et al. (2007d)[19] recently developed a simultaneous calcination and sintering mechanistic model describing pore evolution during cyclic calcination and carbonation. The model was compared with experimental results typically involving 15–16 calcination/carbonation cycles. Pores of diameter <220 nm (labeled Type 1) shrank, whereas pores ≥220 nm (Type 2) grew. Shrinkage of Type 1 pores is an essential feature of solid-state sintering (German, 1996),[20] whereas the growth of Type 2 pores may not occur in all cases, e.g. when the particle size is smaller than the diameter of Type 2 pores. Growth of Type 2 pores is much less important than loss of Type 1 pores because the latter contain much more surface area per pore volume.

In the model of Sun et al. (2007d),[19] only Type 1 pores participate in carbonation. After a certain number of calcination/carbonation cycles, the calcine contains pores of both Types 1 and 2 as a result of sintering during cycling between calcination and carbonation. This contrasts with the ideal sintering-free calcination, or "green stage" (German, 1996),[20] which, during calcination, produces pores of the largest surface area attainable. Upon completion of the next carbonation, only Type 1 pores are filled because Type 2 pores are relatively unreactive during the fast stage of carbonation. Upon further calcination, some Type 1 pores shift to Type 2, resulting in loss of Type 1 pores and possible growth of Type 2 pores. The loss of Type 1 pores leads to reduction in $CO_2$ capture ability during cycling, but with much slower decay rates after many cycles because of the decreasing surface area for sintering kinetics. Experimental studies are needed for extended calcination and carbonation cycling, because, from a practical application point of view, thousands of cycles are likely to be needed (Abanades et al., 2004b).[12] The objective of this work was to determine whether the CaO conversion will approach zero after many calcination/carbonation cycles, or instead approach a nonzero asymptotic value. In addition, we investigate which factors influence the asymptotic capture level and the mechanism governing the observed capture performance. These matters are of critical importance for the design of calcination/carbonation processes.

In applications of CaO in sorption-enhanced steam methane reforming (SMR), solid-state reactions between CaO and common Ni-based SMR support $Al_2O_3$ are possible under typical reforming conditions. High-temperature solid-state reactions between $Al_2O_3$ and CaO have been found when modifying natural-limestone-derived calcines (Sun, 2007)[18] and during dry reforming (Agnelli et al., 1987; Goula et al., 1996a,b).[23–25] Products of $Al_2O_3$–CaO reactions include $CaAl_4O_7$, $CaAl_2O_4$, and $Ca_{12}Al_{14}O_{33}$, with the latter being the major one in most cases. Although Ortiz and Harrsion (2001)[5] did not find appreciable interactions between dolomite-derived CaO and $\gamma$-$Al_2O_3$ as SMR catalyst support in multiple-cycle fixed-bed reforming tests, experiments are also needed to investigate whether there are interactions between CaO and $\gamma$-$Al_2O_3$ in extended cycling and the possible effect on reversibility.

Because this work focuses on experimental investigation of cyclic capture, some relevant results from previous studies are first summarized:

(a) It would appear that alternative limestone-derived sorbents show similar cyclic behavior, especially when the number of cycles is extended (Abanades, 2002; Sun et al., 2007a).[9,14]

(b) The reversibility of limestone-derived sorbents is insensitive to some operating parameters such as carbonation temperature, carbonation pressure and calcination holding time, providing that complete calcination is achieved during each cycle (Grasa and Abanades, 2006; Sun et al., 2007a).[9,26]

(c) Grasa and Abanades (2006)[26] and Lysikov et al. (2007)[27] found that calcium-based sorbents show asymptotic CaO utilizations of ~7.5–15% for both natural limestones and synthetic sorbents.

## Experimental Details

Strassburg limestone was selected as a representative sorbent for this calcination/carbonation cycling study, as it has already been tested intensively for $CO_2$ capture (Sun, 2007; Sun et al., 2007a–d),[9–11,18,19] as well as in $SO_2$ capture studies (Laursen et al., 2000, 2001).[28,29] This limestone contains 96% $CaCO_3$ by weight. Its chemical composition is given elsewhere (Sun et al., 2007d).[19] For all tests in this study, the limestone particles were pre-screened to 212–250 $\mu$m.

An atmospheric fixed-bed thermogravimetric reactor, detailed elsewhere (Laursen et al., 2000, 2001),[28,29] was used in this work. An inert sample holder made of Pd alloy contained the samples. Mass flow controllers were utilized to achieve the desired inlet gas concentrations. The temperature was maintained at 850 ± 3°C for both carbonation and calcination, except where specified otherwise. Because of the insensitivity of sorbent reversibility to carbonation temperature (Grasa and Abanades, 2006; Lysikov et al., 2007; Sun et al., 2007a),[9,26,27] conclusions from these tests should also apply to other test conditions. Carbonation and calcination were mostly carried out in ~1100 ml/min flows of 100% $CO_2$ and 100% $N_2$, respectively. Fresh 500 ± 2 mg fresh limestone samples were loaded into the basket at the start of each run, except where specified otherwise. A 1:1 mass ratio mixture of commercial SMR catalyst (Ni over $Al_2O_3$ support) and Strassburg limestone was also cycled between carbonation and calcination to simulate a sorbent-enhanced SMR system containing intermingled catalyst and sorbent.

With the sample size and gas flow rate in this study, the reactor may not achieve differential reactor conditions. However, because we focus on cyclic calcium utilization behavior that has been found to be insensitive to reactor type and sample loading (Sun et al., 2007d),[19] the conclusions reached in this work should be transferable to other cases, except that the reaction times and rates may be influenced by the nature of the reactor.

Switching between $CO_2$ and $N_2$ was automatically controlled using program-controlled solenoid valves, with pre-determined time intervals for both calcination and carbonation. The actual carbonation time was slightly less than the nominal carbonation time due to piping-related delays in the gas introduction system. In tests where completion of the fast stage of carbonation was desired, completion of calcination at the start of the cycling usually required longer than the selected calcination time (e.g., 9 min). Therefore, the carbonation and calcination times were usually extended in these

**Table 1. Summary of Run Details**

| Run # | Carbonation @ 100% $CO_2$, 850°C | Calcination @ 100% $N_2$, 850°C (Except where Specified Otherwise) | Details, Comments |
|---|---|---|---|
| 1 | 9 min each (except first two cycles*) | 8 min each | 1040 cycles, baseline run |
| 2 | 3.5 min each | 4.5 min each | 1020 cycles |
| 3 | First 67 cycles as in run 1,* followed by steps as in run 2 | First 67 cycles as in run l,* followed by same steps as in run 2 | Combine runs 1 and 2 |
| 4 | First 112 cycles as in run l,* followed by steps as in run 2 | First 112 cycles as in run 1,* followed by same steps as in run 2 | Combine runs 1 and 2 |
| 5 | 9 min each* | First 67 cycles as in run l,* followed by steps of 4.5 min each | Combined run 1 and a run of reduced calcination time |
| 6 | 15 min each | 15 min for first 98 cycles, followed 12 min of calcination | Longer carbonation time than run 1; 303 cycles |
| 7 | | | |
| 7A | 3.5 min each | 4.5 min each | 557 cycles |
| 7B | Started from residues of run 7A. First two cycles same as run 2, followed by ~24 h of carbonation, then cycled with 9 min for each sorption | First two cycles same as for run 2, later cycles of 8 min for each calcination | For mechanism study; long carbonation as a reactivation step; started from run 7A product |
| 7C | Repeat run 7A and long carbonation of run 7B | No calcination | Started from run 4 product, followed by long carbonation |
| 7D | No carbonation | Complete calcination of run 7C sample | Full calcination of run 7C sample |
| 8 | | | |
| 8A | No carbonation | Calcined in 50% $CO_2$ and 50% $N_2$ at 900°C, then held for 24 h | Sintering of initially calcined sample |
| 8B | Started from calcine from run 8A 9 min each | 8 min each | Same as run 1 starting with samples prepared in run 8A, 263 cycles |
| 9 | Started from reduced SMR catalyst and fresh limestone (273 mg in total, catalyst/limestone 1:1 by wt) 9 min each | 8 min each | 221 cycles |

*The first two cycles used longer carbonation time because they needed more than 9 min to complete the fast stage of carbonation.

tests during the first two cycles to complete the fast stage of carbonation.

At the end of each test, solid samples were immediately collected and saved in a desiccator. Selected samples were sent for SEM studies by a HITACHI S-3000 instrument. Before high-resolution SEM measurements, all samples were first gold-coated. A Micromeritics AutoPore IV 9500 Poresizer determined the pore size distributions of selected samples.

## Results and Discussion

Table 1 summarizes the run details. Runs 1 to 6 were designed to test the effect of both calcination time and carbonation time. Run 7 included four steps, with the last two repeating the first two for sampling purposes. This run was intended to reveal the effect of long carbonation as a reactivation step and to provide insight into the mechanism of decay during cycling. Run 8 involved two steps. The first (8A) is to reduce the volume of Type 1 pores by non-cyclic sintering (calcination at 900°C in 50% $CO_2$ and 50% $N_2$ for 24 h) on a fresh calcine, and to produce a sample with diminished capture ability, while avoiding calcination/carbonation cycling. In the second step (8B), the sintered sample was tested under the same conditions as for run 1 to determine whether non-cyclic sintering is equivalent to prolonged cycling in terms of decay of sorbent capture. Note that the starting sample size for run 8A was larger (~800 mg) than normal (~500 mg). Careful sampling was performed for ana-

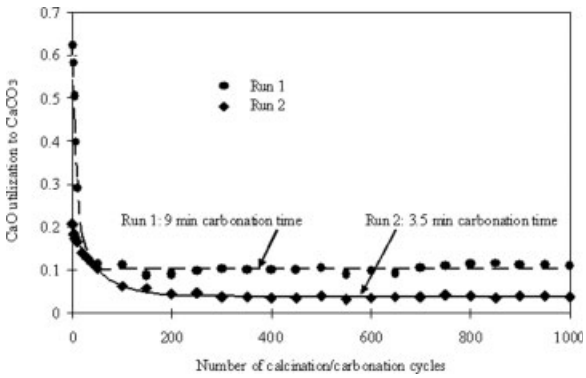


**Figure 1. Cyclic performance of Strassburg-limestone-derived sorbent over 1000 calcination and carbonation cycles: with Eq. 1 fitted lines.**

Every 50th point plotted except at the beginning (calcination times: 8 min run 1 and 4.5 min run 2).

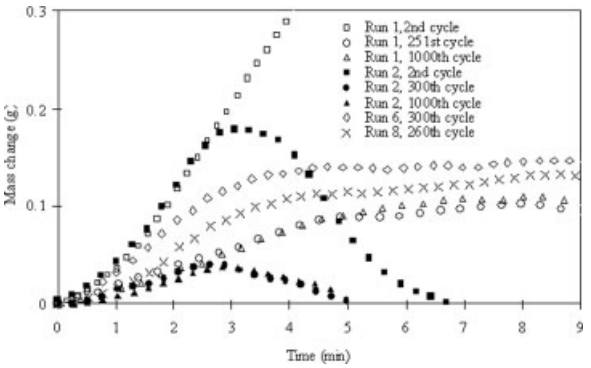


**Figure 2. Mass breakthrough histories for selected cycles of runs 1, 2, and 6.**

For test conditions see Table 1.

lytical purposes after run 8A to ensure that the sample size left for run 8B was the same as for the runs that started with 500 mg limestone.

The 1000-cycle results for runs 1 and 2 are shown in Figure 1. An important finding is that there was a non-zero asymptotic CaO utilization for both cases, as reported by Grasa and Abanades (2006),[26] although the asymptotic levels differ significantly (~10% and ~3.5% for runs 1 and 2 in this work and ~7.5% in the work of Grasa and Abanades (2006)).[26] Lysikov et al. (2007)[27] recently drew a similar conclusion that stable CaO reversibility could be achieved during prolonged cycling, mostly based on one or two hundred cycles for synthetic sorbents, as well as a commercial limestone. The existence of a non-zero asymptotic capture level is good news in that it may make it possible to minimize the addition of fresh make-up sorbent during prolonged operation. It also requires that our previously derived mechanistic model describing cyclic capture be modified. Another important implication of these findings is that the operating conditions appear to affect the asymptotic utilization level, as revealed by the different ultimate capture ability for runs 1 and 2.

Several empirical equations have been employed in earlier work to describe cyclic behavior of calcium-based sorbents. Abanades and Alvarez (2003)[15] proposed $X(n) = a^n(1-b)+b$, with $a = 0.77$ and $b = 0.17$ based on fitting ~20 cycles of experimental data. Wang and Anthony (2005)[30] suggested $X(n) = (1+an)^{-1}$ with $a = 0.24$, again based on ~20 experimental cycles. Sun et al. (2007a)[9] fitted their data by means of $X(n) = a(n+1)^{-b}$ with $a = 1.07$, $b = 0.49$, based on a simultaneous sintering and calcination model. Grasa and Abanades (2006)[26] proposed $X(n) = (1-a)/[1+bn(1-a)]+a$ with $a = 0.075$ and $b = 0.52$ based on their 500-cycle study. However, none of these four forms of equation provided satisfactory fitting for the experimental results obtained in the present work. Instead, all sets of data could be well fitted by an equation with three adjustable parameters of the form

$$X(n) = a \times \exp[-b \times (n-1)] + c \qquad (1)$$

where $X(n)$ is the CaO conversion after the $n$th carbonation and $n$ is the number of cycles. Coefficient $c$ represents the asymptotic (ultimate) value in each case, and hence is of special interest; $(a + c)$ is the initial utilization during the first cycle, whereas $b$ governs the rate of decay. Least-square values of the fitted constants $a$, $b$, and $c$ were 0.529, 0.104, and 0.103 for run 1, and 0.152, 0.018 and 0.038, respectively, for run 2.

To gain more insight into the effect of sorption time, details for selected cycles of runs 1 and 2 are plotted in Figure 2. Note that in run 1 at least, there is no discernible difference in behavior after the 250th cycle. The corresponding carbonation time was long enough to reach the slow (or plateau) stage of carbonation exemplified by the 251st and 1000th cycles. In run 2, the sorbent performed in a very similar manner to its counterpart in run 1. The actual carbonation cycle time was slightly less than the pre-set 3.5 min due to piping-related delays in the gas introduction system. Because the rate of carbonation, represented by the slope for each carbonation stage, should reflect the specific surface area contained by Type 1 pores, runs 1 and 2, when they approach asymptotic calcium utilization, seemingly have similar contents of Type 1 pores, except that there are slightly fewer for run 2 than for run 1.

Because a shorter residence time would be desirable for reactor design, runs 3 and 4, whose results appear in Figure 3, were designed to provide more insight into the effect of carbonation time. Both runs show that once the calcination and carbonation times switched from those of run 1 to the run 2 values, CaO utilization quickly decreased to approach the asymptotic performance of run 2. These runs indicate that the shorter carbonation time is probably the major factor underlying the poorer performance of run 2. These tests also confirm good reproducibility when run 2 conditions were employed.

Run 5 started exactly the same as run 1, but the calcination time was reduced to 4.5 min after 67 cycles. As seen in Figure 4, the reduction in calcination time did not appreciably change the sorbent reversibility. Note, however, that although calcination time had a negligible influence on the asymptotic performance when it was long enough to achieve complete calcination at each step, a previous study (Sun et al., 2007d)[19] showed that the calcination step is very important in terms of sintering and pore evolution because of $CO_2$ outwards diffusion.

The effect of a longer carbonation time can be seen by comparing Figures 2 and 4. Run 6 showed improved CaO utilization, leveling off at ~14% after ~100 cycles. The cal-

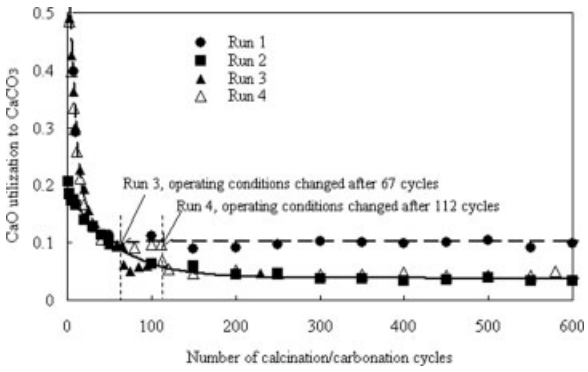


**Figure 3. Cyclic performance of Strassburg-limestone-derived calcine over many calcination and carbonation cycles showing asymptotic $CO_2$ capture levels.**

Lines are fitted from Eq. 1; runs 3 and 4 are compared with run 2. Test conditions appear in Table 1.

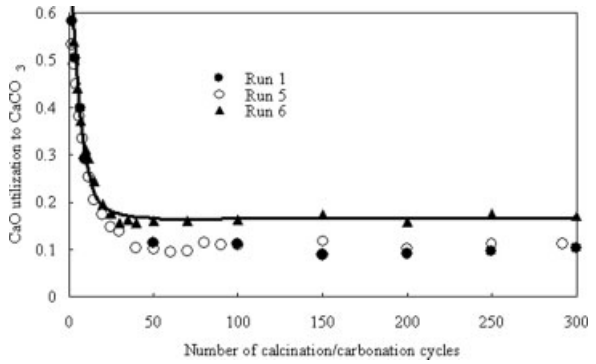


**Figure 4. Cyclic performance of Strassburg-limestone-derived calcine for prolonged calcination and carbonation cycles showing asymptotic $CO_2$ capture levels for runs 5 and 6 compared with run 1.**

Test conditions appear in Table 1. The line is the Eq. 1 fit for run 6.

cination time was reduced to 12 min after 98 cycles to save time, with no visible effect, consistent with the previous finding that the calcination time has no effect on cyclic performance when it was sufficient for complete calcination. The mass changes in Figure 2 show accelerated carbonation in run 6, indicating a higher specific surface area of Type 1 pores in run 6 calcines. The change of carbonation time must have led to a profound change in pore size distribution, altering the ultimate capture ability. As shown in Figure 4, the results of run 6 can again be well fitted by Eq. 1, in this case with $a = 0.554$, $b = 0.158$, and $c = 0.166$.

Run 7 tested a series of steps. The first (7A) began with repeating the calcination and carbonation cycling of run 2 for 557 cycles. The CaO utilization was, as expected, very similar to run 2. After being stored in a desiccator for a few days, this much-cycled sorbent was subjected to two further cycles at the test conditions of run 2 and then carbonated for 24 h in pure $CO_2$ at 850°C. Complete calcination was next performed in $N_2$, and the test conditions of run 1 were then applied, i.e., 9 min carbonation followed by 8 min calcination for each cycle, for 14 cycles (referred as to run 7B). The results are compared with run 1 in Figure 5. The previously cycled sorbent confirmed much reduced capture ability in the initial two cycles of run 7B, but the following 24 h of carbonation achieved ~49% CaO utilization. The cyclic performance then greatly improved, with the performance approaching that of run 1. Apparently the long period of carbonation reactivated the sorbent for further cyclic $CO_2$ capture. Similar reactivation due to long carbonation was reported by Barker (1973)[31] and Salvador et al. (2003),[32] but without explanation. To further elucidate the mechanism, samples were collected after two further steps. Run 7C involved exposing the highly cycled residue from run 4 to 24 h of carbonation, whereas a complete calcination of the carbonated samples from run 7C was carried out in run 7D.

Figure 6a shows a SEM image of initial calcines which apparently lack pores of 500–1000 nm diameter, but have abundant much smaller pores. The findings confirm a previous study for Strassburg limestone of the same particle size (Sun et al., 2007a)[9] and other studies with different limestones (Abanades et al, 2004a; Abanades and Alvarez, 2003; Alvarez and Abanades, 2005).[7,15,33] The pore size distribution for the initial calcine in Figure 7 shows that initial calcines have a peak pore size at <100 nm (Type 1). As seen in Figure 6b, the often-cycled calcines from run 1 appear to have very large (Type 2) pores of mouth diameter ≥1000 nm and an apparent lack of smaller pores. The reduction of carbonation time in run 2 resulted in even larger pores, i.e. ~1000–3000 nm. The existence of these large pores is confirmed by the pore size distribution in Figure 7. In the pore size distribution, intra-particle pores have been approximately differentiated from inter-particle voids based on SEM observation. Larger voids not visible on SEM images are generally considered to be inter-particle voids and are not shown in Figure 7. Neither run 1 nor run 2 showed significant pore volume for pores <350 nm, both in SEM images (Figures 6b, c) and in pore size distribution measurements (Figure 7). Based on the same argument as in our previous work (Sun et al., 2007d), we assume that all samples in this test did not possess pores smaller than 6 nm. However, the residual $CO_2$ capture ability of calcines from runs 1 and 2, as evidenced by the relatively fast carbonation (1000th cycle for run 1 and 300th cycle for run 2), indicates the existence of some Type 1 pores providing accessible surface area for subsequent carbonation. Note that Figure 7 appears to give contrasting observations with calcines generated in Run 1 having more large-pores (~1000 nm) than those from Run 2. However, in this case SEM observations are likely to be more accurate because the pore size distribution measurements could include inter-particle voids (coincidently also in this size range) as intraparticle pores.

Earlier studies on the same limestone (Sun et al., 2007a–d)[9–11,19] and other limestones (Abanades et al, 2004a; Abanades and Alvarez, 2003)[7,15] all showed bimodal pore size distributions with two types of pore, with a clear division at ~220 nm, but these tests typically only lasted for 15–20 cycles. When using the measured Type 1 pores (<220 nm), the equations suggested by Sun et al. (2007d)[19] predict 14.4 and 3.9% utilizations for calcines after runs 1 and 2, compared with the experimental asymptotic CaO utilizations of 10.3 and 3.8%, respectively. The discrepancy is believed to be due to the scattering of pore size distribution data. In pore size distributions for runs 1 and 2 in Figure 7, despite the

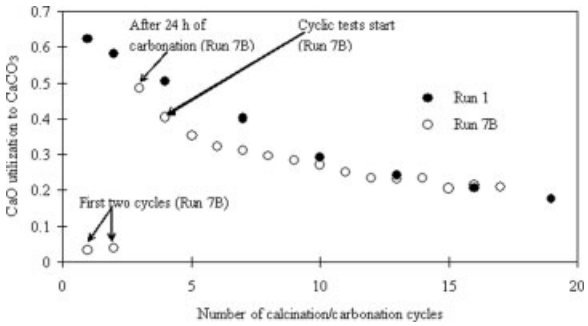


**Figure 5. Test results showing the effect of a 24-h carbonation on cyclic performance: results of run 7B compared with run 1.**

Test conditions appear in Table 1.

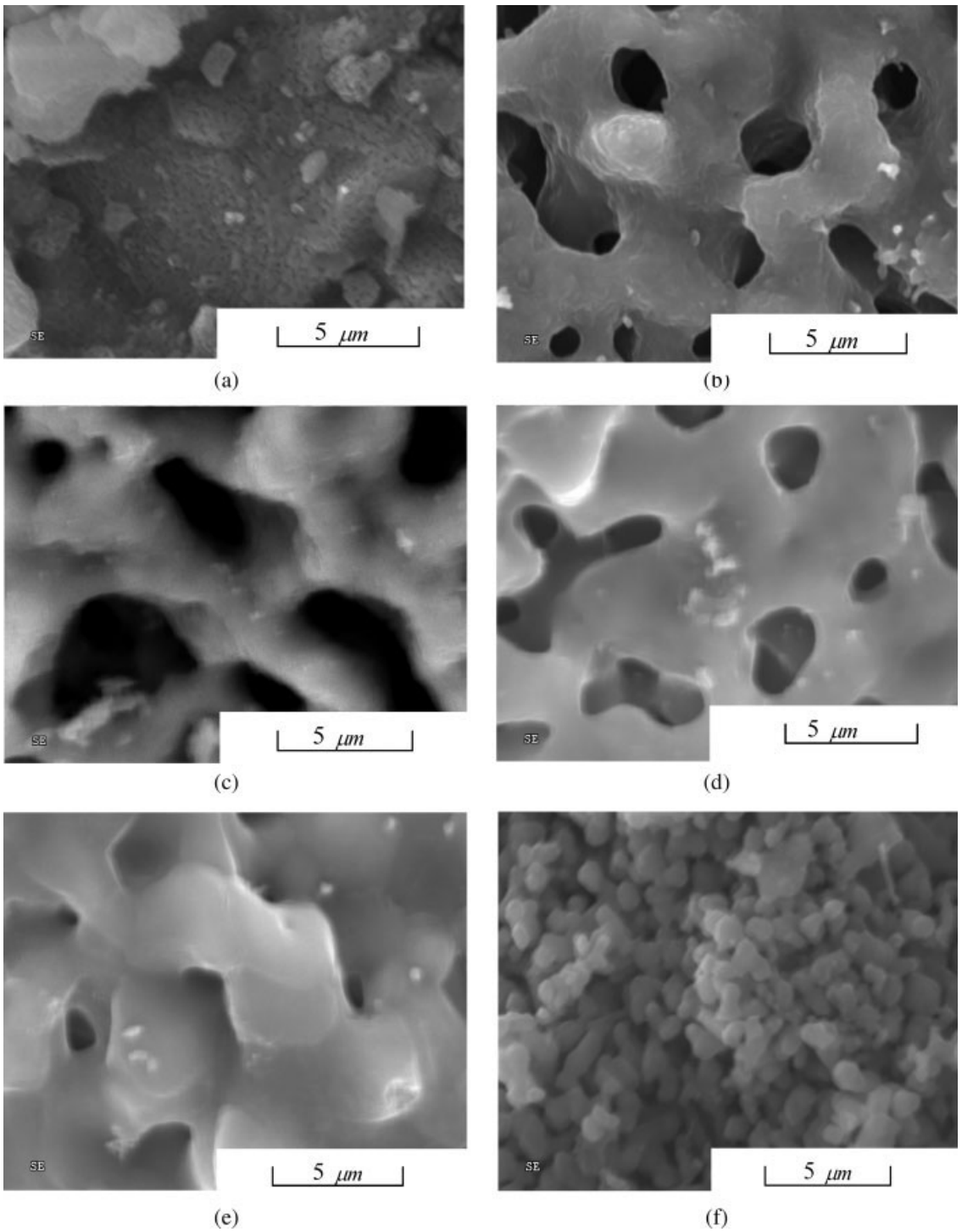


**Figure 6. SEM photos showing surface texture for a variety of samples.**

All samples were derived from 212 to 250 3m Strassburg limestone. (a) Initial calcine; (b) calcines from run 1 after 1040 cycles; (c) calcines from run 2 after 1020 cycles; (d) carbonates from run 7C. Test history: 1000 cycles in run 2 and 24 h carbonation; (e) calcines from run 7D, calcined sample from run 7C; (f) calcines from run 8A after calcination and sintering for 24 h.

small pore volume in the <220 nm range and lack of obvious division between pores smaller than ~350 nm (Figure 7), the predicted trend implies that there are still many Type 1 pores responsible for the observed faster stage of capture. Given the scattering of pore size distribution data, the boundary between Type 1 and Type 2 pores could also be approximated as ~350 nm (rather than 220 nm), because most Type 2 pores are apparently larger than ~350 nm for all of the often-cycled sorbents. The results also imply that the reduction of $CO_2$ capture ability in run 2 is not merely because of reduced carbonation time, but mostly due to structural change of the pores.

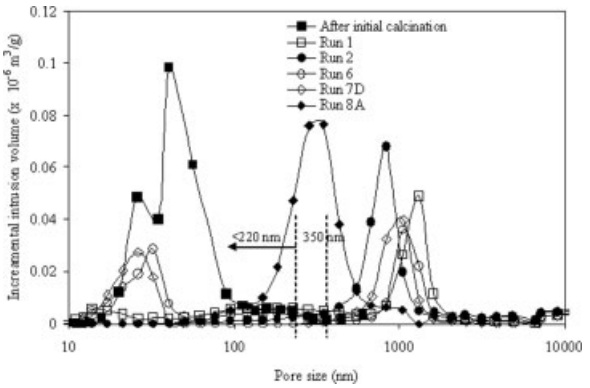


**Figure 7. Pore size distributions determined by mercury intrusion method.**

Samples after initial calcination for runs 1, 2, 6, 7D, and 8A.

The surface texture of the carbonated sample from run 7C is shown in Figure 6d. Because run 7C started from the often-cycled samples from run 7A, one might expect a similar texture as in Figure 6c before the long carbonation. Figure 6d shows that after reaching ~49% calcium utilization, the sorbent surface had become very smooth, suggesting the filling of all Type 1 pores. There was also a reduction in pore mouth diameters for the larger Type 2 pores caused by swelling, with the molar volume of $CaCO_3$ ~2.17 times that of CaO. The calcine after the long carbonation (run 7D) shown in Figure 6e shows a major reduction in Type 2 pores relative to its original condition before the long carbonation illustrated in Figure 6c. Type 1 pores in run 7D calcines cannot be clearly viewed in Figure 6e. However, their existence is clearly shown in the pore size distribution of Figure 7 with a peak at <100 nm. It can be concluded that reactivation by long carbonation is very effective in re-arranging pores. It can also be deduced that carbonation and subsequent calcination make the pores involved in the long carbonation (both Types 1 and 2) "forget" their previous cycling history. The extent to which the much less reactive Type 2 pores are involved in each carbonation (determined by carbonation time), determines the different observed surface textures. In Figures 6e and 7, there are still some Type 2 pores in the calcines after long carbonation, indicating that 24 h of reactivation by carbonation was not long enough to rearrange all Type 2 pores.

These test results suggest that the carbonation time should be as long as possible to maximize the utilization of Type 2 pores. Long carbonation times are desired from the beginning of cycling to improve the capture ability. Comparing the results from runs 1 and 6 in Figures 2 and 4, one apparently can benefit from longer carbonation, not merely from higher ultimate capture level, but also from a higher carbonation rate, as evidenced by the higher slope for run 6 in Figure 2. These improvements appear to be due to better-preservation of Type 1 pores, as shown by the measured pore size distribution of run 6 calcines in Figure 7. However, in practice, prolonged carbonation is unlikely to be commercially economical because a greater portion of the carbonation time would correspond to the very slow carbonation stage. Hence a balance is needed to optimize the residence time in a carbonator.

Run 8 was undertaken to determine whether or not the cyclic time needed to approach the asymptotic capture level could be reduced. The calcination stage lasted 24 h in the presence of both $CO_2$ and $N_2$ (run 8A), but the cycling was otherwise the same as for run 1. The results are shown in Figure 8. The best fit values of $a$, $b$, and $c$ from Eq. 1 were 0.157, 0.036 and 0.131, respectively. The considerable reduction in calcium utilization at the early stage of cycling was due to a sintering-related reduction in surface area that should involve a decrease in Type 1 pores. The surface texture of the sintering calcine in Figure 6f shows remarkable grain growth compared with the initial calcines in Figure 6a. The pore size distribution for sintered calcines in Figure 7 features single-peaked enlarged pores distributed from 100 to 1000 nm. Compared with the bimodal pore size distribution normally observed for much-cycled samples, calcines held for prolonged time in $N_2$ in our previous study (Sun et al., 2007d) or in $N_2 + CO_2$ as in the present study, only resulted in a pore size shift, but still with a single peak, indicating mechanistic differences between sintering by cycling and by simply holding for a long time.

When the cycling started in run 8B, the capture for the 2nd cycle was somewhat higher than for the 1st cycle. The utilization then slowly leveled off after 100 cycles, reaching ~13–14% calcium utilization. The gradual decay of the capture ability can be attributed to slow sintering kinetics due to reduced specific surface area because of a reduction in Type 1 pores (Sun et al., 2007d).[19] The mass breakthrough details in Figure 2, however, show that when the asymptotic level is closely approached at cycle 260 of run 8, the carbonation slope remained higher than for run 1, indicating the retention of many Type 1 pores. SEM images for the cycled samples (not shown here) after completing run 8B showed very similar texture as in Figure 6b, with apparent type 2 pores. This implies that during cycling of sorbents from run 8A, a similar pore evolution mechanism applied, producing both Type 1 and Type 2 pores. This test also demonstrates that pre-treatment can reduce the required residence time from the beginning of cycling, while maintaining higher ultimate capture.

The reversibility of CaO interspersed with a commercial SMR catalyst (Ni on $Al_2O_3$) is shown in Figure 8. Because

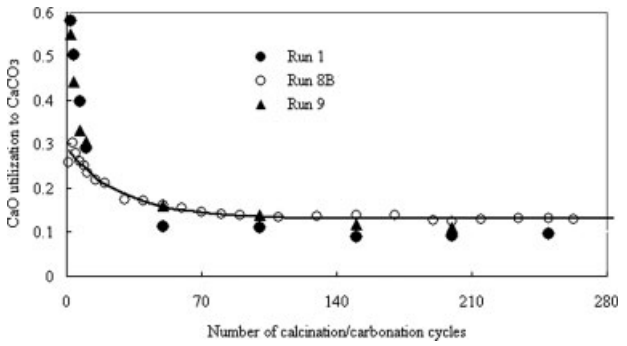


**Figure 8. Cyclic performance of Strassburg-limestone-derived calcine over many calcination and carbonation cycles showing asymptotic $CO_2$ capture levels: results of runs 8B and 9 compared with run 1.**

Test conditions appear in Table 1. The line is the Eq. 1 fit for run 8B.

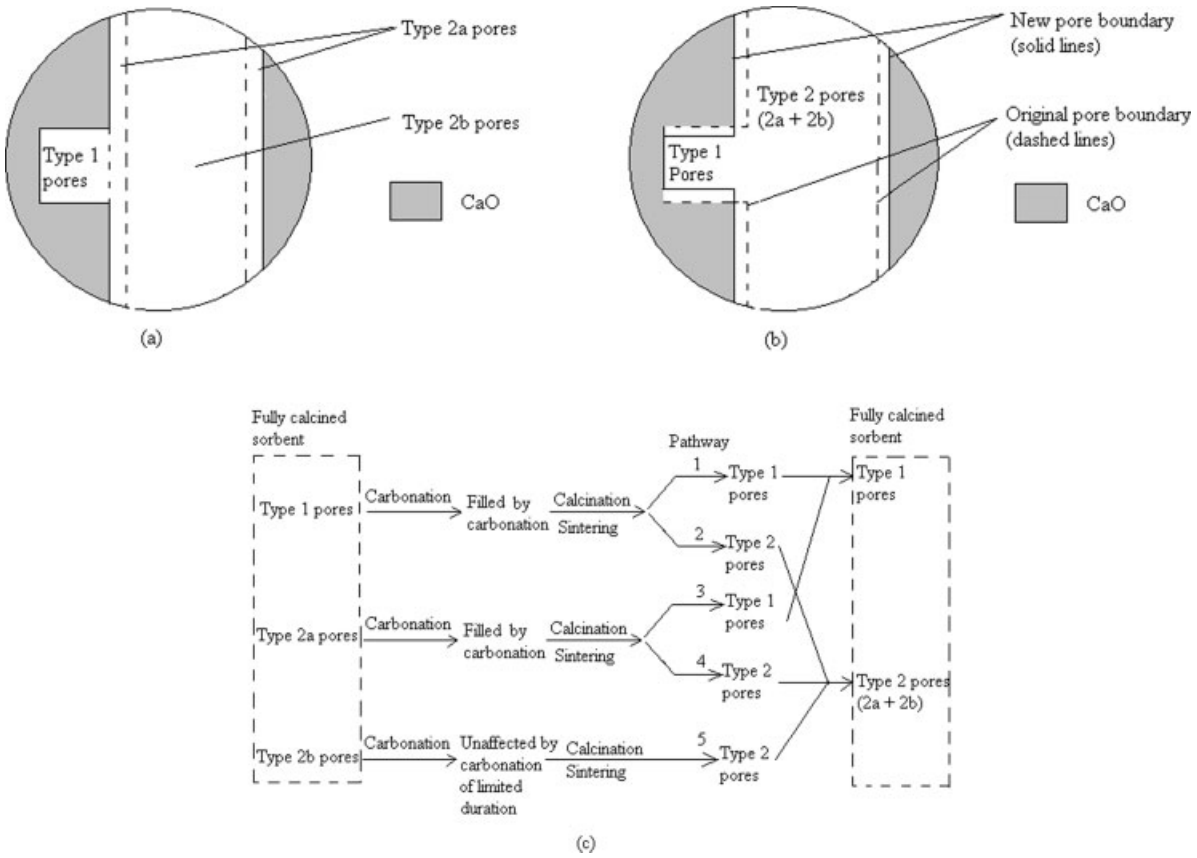


**Figure 9. Schematic representation of modified pore evolution mechanism during cyclic calcination and carbonation.**

(a) Original division of Type 1 and Type 2 pores for a fully calcined sorbent; (b) division of Type 1 and Type 2 pores after many carbonation/calcination cycles for a fully calcined sorbent; (c) pathways followed by evolving pores during carbonation and calcination.

of dilution by the catalyst, much less CaO was available in the mixture than in the other runs. The performance after 221 cycles was very similar to that in run 1, indicating that the catalyst did not interfere with the ability of the sorbent to capture $CO_2$. Although CaO was very reactive with bulk $Al_2O_3$ under similar test conditions (Sun, 2007),[18] $Al_2O_3$ as a catalyst support was not reactive with CaO, probably due to a lack of reactive sites and limited contacting between the solid species.

### *Evolution of pores: A plausible mechanism*

The pore-evolution model of Sun et al. (2007d)[19] requires revision to address the non-zero asymptotic (ultimate) CaO utilizations observed in our extended experiments. The proposed modified mechanism based on the experimental observations discussed above is described stepwise and illustrated in Figure 9:

(1) At an early stage of cycling, calcines contain both type 1 and type 2 pores as a result of simultaneous calcination and sintering, as discussed by Sun et al. (2007d).[19] Slightly different from what was assumed in the previous model (Sun et al., 2007d)[19] to accommodate the new experimental observations, Type 1 pores may or may not have an obvious peak at $\sim$100 nm, depending on the stage of cycling. Type 2 pores are sub-divided into two parts, as depicted in Figure 9a, with Type 2a representing pores close to the exterior of the particles available for the next step of carbonation, whereas Type 2b pores are not available for the next limited-duration carbonation due to their distance from the exterior, despite having radii similar to Type 2a pores. For longer carbonation times, more Type 2 pores participate in carbonation, resulting in a higher fraction of Type 2a pore volume. Type 1 pores provide almost all the surface area and determine the apparent carbonation rates. The difference between the previous model of Sun et al. (2007d)[19] and this modified version is that Type 2a pores partake in carbonation, though at much reduced reaction rates.

(2) During a complete cycle consisting of one carbonation step and the next calcination period, the three classifications of pores in a fully calcined sorbent, Types 1, 2a, and 2b, experience different evolution histories. During carbonation, only Types 1 and 2a pores are able to accommodate carbonate product, whereas Type 2b pores barely change. When the newly formed carbonate is fully calcined, sintering during calcination re-arranges the pores left behind because of $CO_2$ evolution, as described in Sun et al. (2007d).[19] The pore distribution (see Figure 9b with pore boundaries from the last cycle also marked for comparison) differs from that at the end of previous cycle (Figure 9a), with less Type 1 pore volume during the early stage of cycling. This is consistent with the findings of run 7 which indicate that when pores have

been used to accommodate carbonate, they "forget" their previous cycling history and re-produce Type 1 and Type 2 pores as in the initial calcination step.

(3) This pore evolution mechanism is further depicted in Figure 9c, with five parallel calcination/sintering pathways for the three pore classifications. Both Type 1 and Type 2a pores can accommodate carbonate in subsequent cycles. Upon complete calcination, pores appearing after $CO_2$ release are re-distributed into Type 1 and Type 2 (with both 2a and 2b possible, depending on their availability during the next carbonation step) in accordance with the simultaneous calcination/sintering mechanism (Sun et al., 2007d).[19]

(4) Because during early cycles, Type 1 pores are plentiful, the loss of Type 1 pores due to the production of Type 2a pores via pathway 2 in Figure 9c exceeds the production of Type 1 pores via pathway 3. The net effect of this stage of cycling is a monotonic decrease in the total volume of Type 1 pores, and hence a monotonic decline in carbonation rates and CaO utilization for a fixed carbonation time.

(5) After many cycles and further growth of Type 2 pores at the expense of Type 1 pores, a dynamic equilibrium is approached when the production of Type 2 pores through pathway 2 is balanced by the production of Type 1 pores via pathway 3. After this point is reached, there is no further net reduction of overall type 1 pores during further cycling, and asymptotic capture is achieved. Changing the operating conditions, e.g. calcination temperature, affects the sintering kinetics and the relative importance of different pathways leading to a different ultimate capture levels and different relative fractions of the three types of pores.

This revised mechanism is consistent with the experimental results of this work. In run 2 with reduced carbonation time, less Type 1 pore volume was regenerated than in run 1. On the other hand, run 6 produced much more Type 1 pore volume because more Type 1 pores were involved in each reactivation step. The increase in Type 1 pores in run 6 is also consistent with the increased carbonation rate for run 6 in Figure 2. The slight improvement in cyclic performance for run 8 and in its carbonation rate relative to run 1 may be due to improved pore distribution achieved by the initial presintering, resulting in either somewhat more Type 1 pore volume via pathway 3, or less Type 2a pore volume via pathway 2. Further quantitative modeling is needed to gain more insight and to find the optimal cycling conditions.

## Conclusions

Asymptotic non-zero capture was attained with a limestone for all conditions tested, in some cases involving more than 1000 cycles, always in the absence of $SO_2$. The ultimate CaO utilization level depended on the operating conditions, especially the carbonation time. Changing the carbonation and calcination conditions caused the sorbent to approach the ultimate utilization which would have been achieved if the new conditions had been in place from the beginning. With the help of SEM and pore size distribution measurements, the results are consistent with a mechanistic model extended from Sun et al. (2007d)[19] where carbonation, combined with the following calcination, serves as a reactivation step, altering the pore distribution between Type 1 ($\leq$220–350 nm) and Type 2 ($\geq$220–350 nm) pores. An important feature of this modified mechanism is that a portion of Type 2 pores are involved in each carbonation stage, contributing to reactivation by producing some Type 1 pores.

## Acknowledgments

The authors are grateful to Dr. Zhongxiang Chen and Mr. Hoon sub Song for assistance with the experiments, and to Dr. Ben Anthony for useful discussions. Funding was provided by the Natural Sciences and Engineering Research Council of Canada and by Tokyo Gas.

## Literature Cited

1. Han C, Harrison DP. Simultaneous shift reaction and carbon dioxide separation for the direct production of hydrogen. *Chem Eng Sci*. 1994;49:5875–5883.
2. Johnsen K, Ryu HJ, Grace JR. Lim CJ. Sorption-enhanced steam reforming of methane in a fluidized bed reactor with dolomite as $CO_2$-acceptor. *Chem Eng Sci*. 2006;61:195–1202.
3. Lin S-Y, Suzuki Y, Hatano H, Harada M. Hydrogen production from hydrocarbon by integration of water-carbon reaction and carbon dioxide removal (HyPr-RING Method). *Energy Fuels*. 2001;15: 339–343.
4. Lin S-Y, Suzuki Y, Hatano H, Harada M. Developing an innovative method, HyPr-RING, to produce hydrogen from hydrocarbons. *Energy Convers Manage*. 2002a;43:1283–1290.
5. Ortiz AL, Harrison DP. Hydrogen production using sorption-enhanced reaction. *Ind Eng Chem Res*. 2001;40:5102–5109.
6. Abanades, JC, Alvarez D, Anthony EJ, Lu D. In-situ capture of $CO_2$ in a fluidized bed Combustor. In Proceedings of the 17th Inter Fluidized Bed Combustion Conference, Jacksonville, Florida, USA, 2003, paper 10.
7. Abanades JC, Anthony EJ, Alvarez D, Lu D, Salvador C. Capture of $CO_2$ from combustion gases in a fluidized bed of CaO. *AIChE J*. 2004a;50:1614–1622.
8. Shimizu T, Hirama T, Hosoda H, Kitano K, Inagaki M. Tejima, K. *A twin fluid-bed reactor for removal of $CO_2$ from combustion processes Trans IChemE*. 1999;77:62–68.
9. Sun P, Grace JR, Lim CJ, Anthony EJ. Removal of $CO_2$ by calcium-based sorbents in the presence of $SO_2$. *Energy Fuels*. 2007a;21:163–170.
10. Sun P, Grace JR, Lim CJ, Anthony EJ. Sequential capture of $CO_2$ and $SO_2$ at FBC conditions. *Environ Sci Technol*. 2007b;41:2943–2949.
11. Sun P, Grace JR, Lim CJ, Anthony EJ. Co-capture of $H_2S$ and $CO_2$ in a pressurized gasifier based process. *Energy Fuels*. 2007c;21:836–844.
12. Abanades JC, Rubin ES, Anthony EJ. Sorbent cost and performance in $CO_2$ capture system. *Ind Eng Chem Res*. 2004b;43:3462–3466.
13. Silaban A, Narcida M, Harrison DP. Characteristics of the reversible reaction between $CO_2$(g) and calcined dolomite. *Chem Eng Commun*. 1996;146:149–162.
14. Abanades JC. The maximum capture efficiency of $CO_2$ using a carbonation/calcination cycle of CaO/$CaCO_3$. *Chem Eng J*. 2002;90:303–306.
15. Abanades JC, Alvarez D. Conversion limits in the reaction of $CO_2$ with lime. *Energy Fuels*. 2003;17:308–315.
16. Borgwardt RH. Sintering of nascent calcium oxide. *Chem Eng Sci*. 1989a;44:53–60.
17. Borgwardt RH. Calcium oxide sintering in atmospheres containing water and carbon dioxide. *Ind Eng Chem Res*. 1989b;28:493–500.
18. Sun P. $CO_2$ removal from energy systems using calcium-based sorbents, PhD thesis, University of British Columbia, 2007.
19. Sun P, Grace JR, Lim CJ, Anthony EJ. On effect of CaO sintering on cyclic $CO_2$ capture in energy systems. *AIChE J*. 2007d;53:2432–2442.
20. German RM. *Sintering Theory and Practice*. New York: Wiley, 1996.
21. Beruto D, Barco L, Searcy AW. $CO_2$-catalyzed surface area and porosity changes in high-surface area CaO aggregates. *J Am Cer Soc*. 1984;67:512–515.
22. Ewing J, Beruto L, Searcy AW. The nature of CaO produced by calcite powder decomposition in vacuum and in $CO_2$. *J Am Cer Soc*. 1979;62:580–584.

23. Agnelli ME, Demicheli MC, Ponzi EN. Catalytic deactivation of methane steam reforming catalysts 1. Activation. *Ind Eng Chem Res*. 1987;26:1704–1707.
24. Goula MA, Lemonidou AA, Efstathiouy AM. Characterization of carbonaceous species formed during reforming of $CH_4$ with $CO_2$ over Ni/CaO-$Al_2O_3$ catalysts studied by various transient techniques. *J Catalysis*. 1996a;161:626–640.
25. Goula MA, Lemonidou AA, Griinert W, Baerns M. Methane partial oxidation to synthesis gas using nickel on calcium aluminate catalysts. *Catalysis Today*. 1996b;32:149–156.
26. Grasa GS, Abanades JC. $CO_2$ Capture capacity of CaO in long series of carbonation/calcination cycles. *Ind Eng Chem Res*. 2006; 45:8846–8851.
27. Lysikov AI, Salanov AN, Okunev AG. Change of $CO_2$ carrying capacity of CaO in isothermal recarbonation-decomposition cycles. *Ind Eng Chem Res*. 2007;46:4633–4638.
28. Laursen K, Duo W, Grace JR, Lim J. Sulphation and reactivation characteristics of nine limestones. *Fuel*. 2000;79:153–163.
29. Laursen K, Duo W, Grace JR, Lim J. Characterization of steam reactivation mechanisms in limestones and spent calcium sorbents. *Fuel*. 2001;80:1293–1306.
30. Wang J, Anthony EJ. On the decay behavior of the $CO_2$ absorption capacity of CaO-based sorbents. *Ind Eng Chem Res*. 2005;44:627–629.
31. Barker R. The reversibility of the reaction $CaCO_3 \rightleftarrows CaO + CO_2$. *J Appl Chem Biotechnol*. 1973;23:733–742.
32. Salvador C, Lu D, Anthony EJ, Abanades JC. Enhancement of CaO for $CO_2$ capture in an FBC environment. *Chem Eng J*. 2003;96:187–195.
33. Alvarez D, Abanades JC. Pore-size and shape effects on the recarbonation performance of calcium oxide submitted to repeated calcination/recarbonation cycles. *Energy Fuels*. 2005;9:270–278.

*Manuscript received Sep. 4, 2007, revision received Dec. 3, 2007, and final revision received Feb. 21, 2008.*